引用格式：GUO Xin, SHI Feng, JIA Tiantian, et al. Effect of Incident Light Scattering at AlGaAs Window Layer Interface on Resolution of Transmission-mode GaAs Photocathode[J]. Acta Photonica Sinica, 2023, 52(8):0812001
郭欣，石峰，贾甜甜，等. 入射光在AlGaAs窗口层界面散射对透射式GaAs光电阴极分辨力的影响[J]. 光子学报，2023，52(8)：0812001

入射光在AlGaAs窗口层界面散射对透射式GaAs光电阴极分辨力的影响

郭欣[1,2]，石峰[2]，贾甜甜[2]，张若愚[2]，程宏昌[2]，张益军[3]
（1 北京理工大学 光电学院，北京 102401）
（2 微光夜视技术重点实验室，西安 710065）
（3 南京理工大学 电子工程与光电技术学院，南京 210094）

摘　要：为研究透射式GaAs光电阴极在不同波长入射光环境下的图像分辨能力，提出了一种基于散射传递函数的AlGaAs窗口层界面散射理论模型。制作了透射式GaAs光电阴极，利用不同波长入射光散射传递函数和点扩散函数变化，基于有参峰信噪比拟合对AlGaAs窗口层界面散射引起的入射光学图像退化程度进行了定量分析。结果表明，在相同的粗糙度下随着入射光波长的增加，入射光学图像的能量损失越小，成像质量越高，而三代微光像增强器不同波长入射光测试条件下极限分辨力变化趋势与仿真计算结果一致，可为后续提高透射式GaAs光电阴极分辨力提供了技术支撑。

关键词：光电阴极；GaAs；散射传递函数；波长；粗糙度；分辨力
中图分类号：TN233　　**文献标识码**：A　　**doi**：10.3788/gzxb20235208.0812001

0　引言

负电子亲和势（Negative Electron Affinity，NEA）GaAs光电阴极是目前最有前景的Ⅲ-Ⅴ半导体光电阴极，在微光夜视、激光距离选通成像、激光定位等领域有广泛的应用[1-5]。根据透射式NEA GaAs光电阴极的光电发射理论[6-7]，入射光携带的光学图像需要先经过AlGaAs窗口层，才能被GaAs光电发射层吸收并转化为光电子图像。因此对于透射式NEA GaAs光电阴极，光子和光电子在传输过程中的空间弥散均会直接影响光电阴极的分辨力，空间弥散越小，光电阴极的分辨力则越高。研究者们主要针对光电子空间弥散对透射式NEA GaAs光电阴极的影响开展了研究[8-10]。结果表明，光电子的电离受主散射是其向阴极表面输运过程中发生横向扩散的主要原因，与光电发射层的厚度、电子扩散长度和掺杂浓度等参数密切相关[11-12]。通过变掺杂或变组分结构设计引入的能带变化可形成一个有利于光电子向阴极表面输运的内建电场，从而减小光电子的横向扩散，提高光电阴极的分辨力。然而，在入射光子转化为光电子之前，入射光在AlGaAs窗口层界面散射不可避免会导致能量的损失，降低光学图像的分辨力，并将传递给后级光电子图像，从而进一步恶化透射式NEA GaAs光电阴极分辨力。

基于目前透射式NEA GaAs光电阴极的AlGaAs窗口层界面散射分析缺少理论模型支撑的现状，本文设计了一种基于散射传递函数（Scattering Surface Transfer Function，STF）的AlGaAs窗口层界面散射分析模型，仿真得到在相同表面粗糙度下不同波长入射光的STF和点扩散函数（Point Spread Function，PSF），并利用有参峰信噪比反映AlGaAs窗口层界面散射导致的光学图像退化程度，进一步对不同入射光条件下三代微光像增强器的极限分辨力进行测试试验，验证分析模型的有效性。

基金项目：国家自然科学基金(No. 61771245)，国防工业技术发展计划(No. JCKY2018208B016)
第一作者：郭欣，guoxinkakaxi@126.com
通讯作者：石峰，shfys@126.com
收稿日期：2022-12-05；**录用日期**：2023-01-16

1 AlGaAs窗口层界面散射模型

GaAs光电阴极材料采用多层异质外延材料，主要包括GaAs衬底、AlGaAs腐蚀阻挡层、GaAs光电发射层、AlGaAs窗口层和GaAs盖层，典型结构如图1(a)所示。其中，设计GaAs盖层的目的主要是为了避免GaAs光电阴极材料可能发生的化学污染和机械损伤。因此，在制备透射式GaAs光电阴极时，需要采用湿法化学蚀刻去除GaAs光电阴极材料表面的GaAs盖层，露出AlGaAs窗口层，然后制备一层光学增透膜，如图1(b)所示。由于AlGaAs窗口层存在一定的表面粗糙度，故入射光传输过程中会在该界面发生散射，如图1(c)所示。

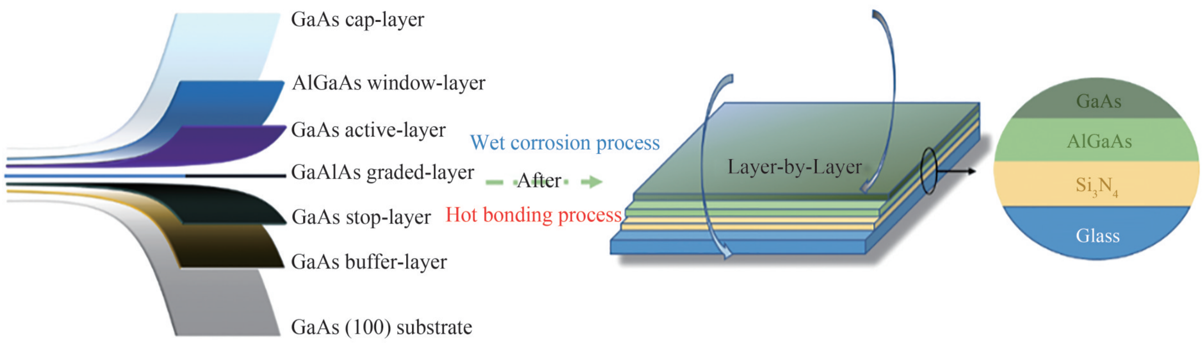

(a) GaAs photocathode structure (b) Transmission-mode GaAs photocathode structure

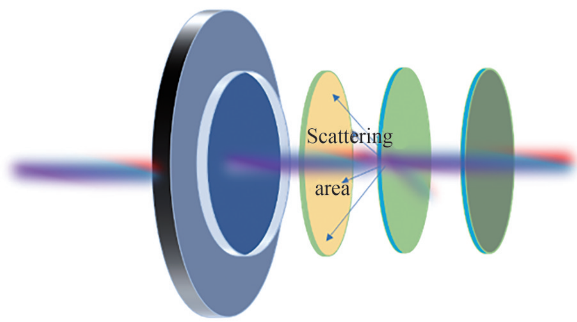

(c) Diagram of window layer interface scattering

图1 GaAs光电阴极制作工艺及AlGaAs窗口层界面散射示意图

Fig. 1 GaAs photocathode fabrication process and AlGaAs window layer interface scattering diagram

假设AlGaAs窗口层粗糙表面随机、高度服从高斯分布且入射光线垂直入射时，STF的计算公式为[13-14]

$$\mathrm{STF}=\exp\left\{-(4\pi\sigma)^2\left|1-\frac{\mathrm{ACV}(\bar{x},\bar{y})}{\sigma^2}\right|\right. \tag{1}$$

式中，σ为AlGaAs窗口层粗糙表面高度分布标准差，σ^2表示粗糙表面高度分布方差，$\mathrm{ACV}(\bar{x},\bar{y})$表示二维表面自相关函数，系数$\bar{x}=x/\lambda$，$\bar{y}=y/\lambda$，$x$和$y$为AlGaAs窗口层的二维方向的长度，$\lambda$表示入射光波长。

对于粗糙表面随机、高度服从高斯分布的AlGaAs窗口层粗糙表面，二维表面自相关函数表示粗糙表面任意两点之间的关联程度，其定义为[15]

$$\mathrm{ACV}(\bar{x},\bar{y})=\sigma^2\left(1/\exp\left(\frac{x/\lambda}{l_x^2}+\frac{y/\lambda}{l_y^2}\right)\right) \tag{2}$$

式中，l_x和l_y分别表示x和y方向上的相关长度。而相关长度进一步可以通过相关系数计算求解，即[15]

$$\rho(x,y)=\frac{E\left[z(x,y)z(x+\Delta x,y+\Delta y)\right]}{\sigma^2} \tag{3}$$

相关系数$\rho(x,y)=1/\mathrm{e}$时的Δx、Δy为表面相关长度，记为l_x和l_y；$z(x,y)$为(x,y)位置处的起伏高度值。

将二维粗糙表面特征参数代入至式(1)，得到关于AlGaAs窗口层表面处的$\mathrm{STF}_{\mathrm{AlGaAs}}$表达式为

$$\mathrm{STF}_{\mathrm{AlGaAs}}=\exp\left\{-(4\pi\sigma)^{2}\left|1-\exp\left(\frac{x}{\lambda l_{x}^{2}}+\frac{y}{\lambda l_{y}^{2}}\right)\right|\right. \tag{4}$$

2　结果和分析

2.1　AlGaAs窗口层粗糙表面自相关函数计算

利用湿法化学蚀刻去除GaAs光电阴极材料表面的GaAs盖层，暴露出AlGaAs窗口层。然后采用原子力显微镜（Atomic Force Microscopy，AFM）（BRUKER MULTIMODE）测试了AlGaAs窗口层的表面粗糙度。测试使用的工作模式为轻叩模式，测试面积为100 μm×100 μm，分辨率为256×256，结果如图2(a)所示。测试结果表明，AlGaAs窗口层表面的平均粗糙度R_a为0.51 nm，均方根粗糙度R_q为1.25 nm。将表面粗糙度矢高分布直方图进行拟合，如图2(b)所示，可以看出其表面粗糙度分布近似满足高斯分布，因此可以用统计光学理论研究AlGaAs窗口层表面粗糙度对成像质量的影响，并为后续高斯粗糙表面[15]的模拟提供条件。

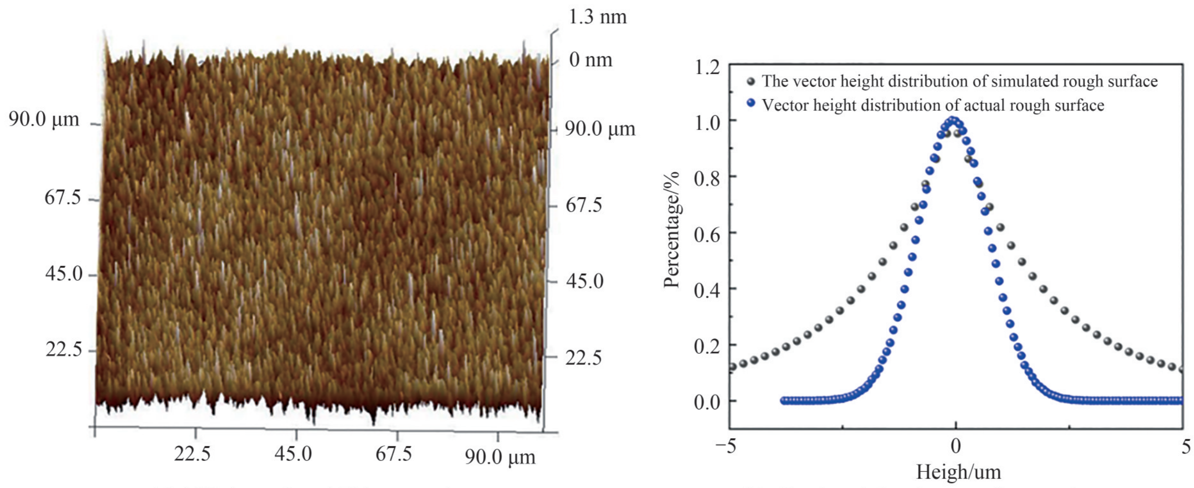

(a) AlGaAs surface AFM test results

(b) AlgaAs window layer surface roughness vector height distribution fitting

图2　AlGaAs窗口层表面粗糙度分布情况

Fig. 2　Surface roughness distribution of AlGaAs window layer

根据已知测试结果得到窗口层粗糙表面标准差值σ=1.25 nm，且其高斯表面分布呈各向同性，则计算得到的自相关长度$l_x=l_y=3$。给予不同的相关长度与均方根粗糙度可以获得不同程度的面型分布，如图3所示。

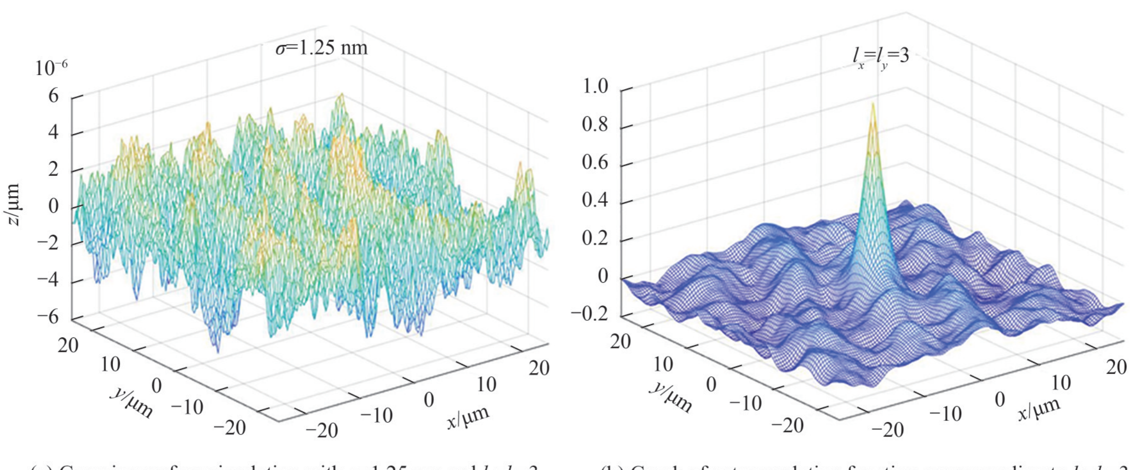

(a) Gaussian surface simulation with σ=1.25 nm and $l_x=l_y=3$

(b) Graph of autocorrelation function corresponding to $l_x=l_y=3$

图3　高斯分布粗糙表面模拟结果

Fig.3　Gaussian distribution rough surface simulation result

2.2 散射传递函数和点扩散函数的计算

为了探讨入射光波长对STF和PSF的影响，将入射光的波长分别设置为530 nm、700 nm和830 nm，并计算了对应波长下AlGaAs窗口层粗糙表面的STF，如图4所示。可以发现，随着入射光波长从550 nm逐步增大至850 nm，STF曲线所包围的积分面积也逐渐增大。这表明，在AlGaAs窗口层表面均方根高度一定时，随着入射光波长的降低，入射光的散射将逐渐变强，STF的减少表明光学图像信息的容量越小，成像越模糊。

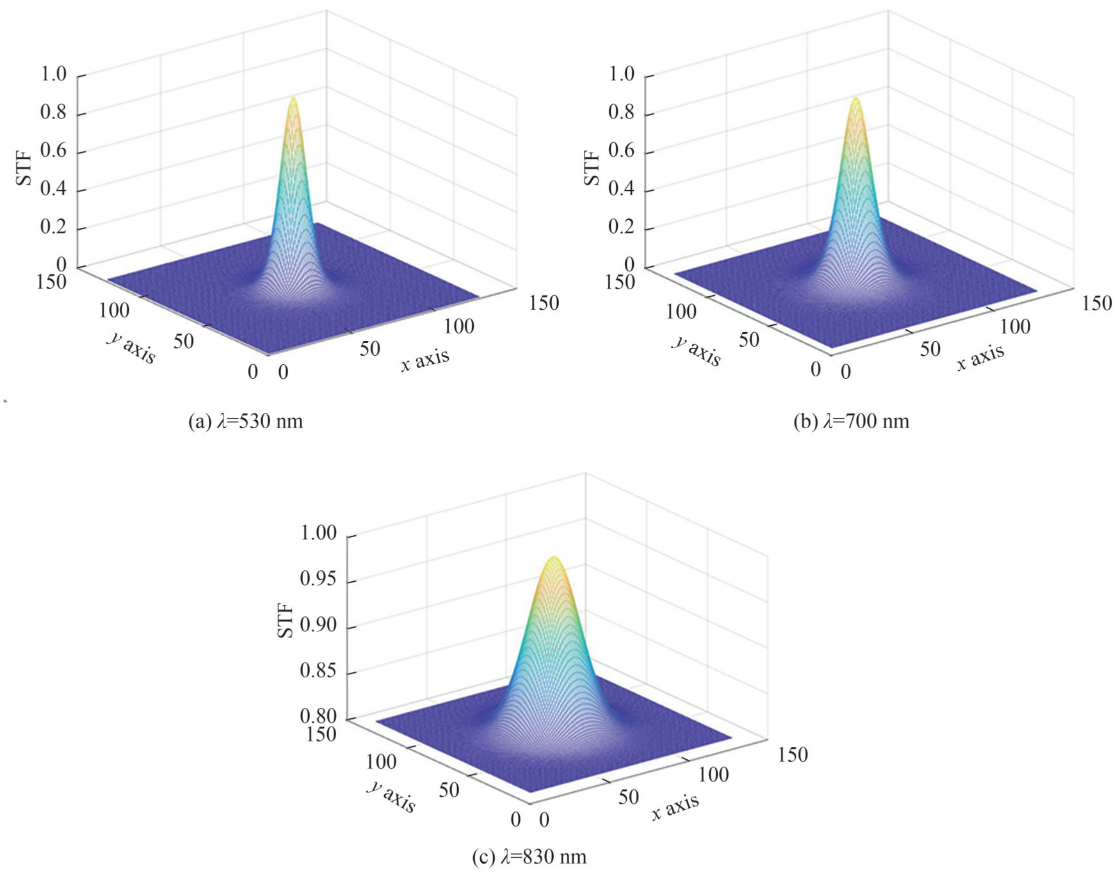

图4 不同入射波长下AlGaAs窗口层粗糙表面的STF函数

Fig.4 STF function of AlGaAs surface window layer rough surface at different incident wavelengths

对STF函数进行Fourier逆变换得出粗糙表面的点扩散函数PSF，图5(a)～(c)为不同波长下AlGaAs窗口层粗糙表面点扩散函数对比图。结果表明，随着入射波长的增加，其点扩散函数中心值增大，即光学图像像面中心能量越集中。此外，在点扩散函数中心以外的小范围内，其值随着波长的减小而增大，且随着半径的逐渐增大，其值的减小速率也逐渐降低，说明光学图像像面的能量随着波长的降低而向外转移，产生亮度逐步增加且尺寸逐步变大的光斑。分析可知，入射光波长的增加可提高能量在光学图像像面上的凝聚能力，入射光波长越大，则能量分布越集中，成像质量越好。

为了定量分析不同入射光波长在AlGaAs窗口层粗糙表面上散射所对应的图像退化程度，采用参数均方误差和参数峰值信噪比(Peak Signal-to-Noise Ratio, PSNR)对图像质量进行评价。峰值信噪比$PSNR_R$公式为[16-17]

$$PSNR_R = 10\log_{10}\frac{K^2}{MSE_R} = 10\log_{10}\frac{N\times M\times K^2}{\sum_{i=1}^{M}\sum_{j=1}^{N}\left[f(i,j)-\hat{f}(i,j)\right]^2} \tag{5}$$

式中，K表示数字图像的量化位数，$M\times N$为图像尺寸，MSE_R为图像有参均方误差，表示退化图像与原始图像之间的差异，$f(i,j)$为原始图像，$\hat{f}(i,j)$为退化后图像。$PSNR_R$数值越大，表示退化图像与原图像差异越

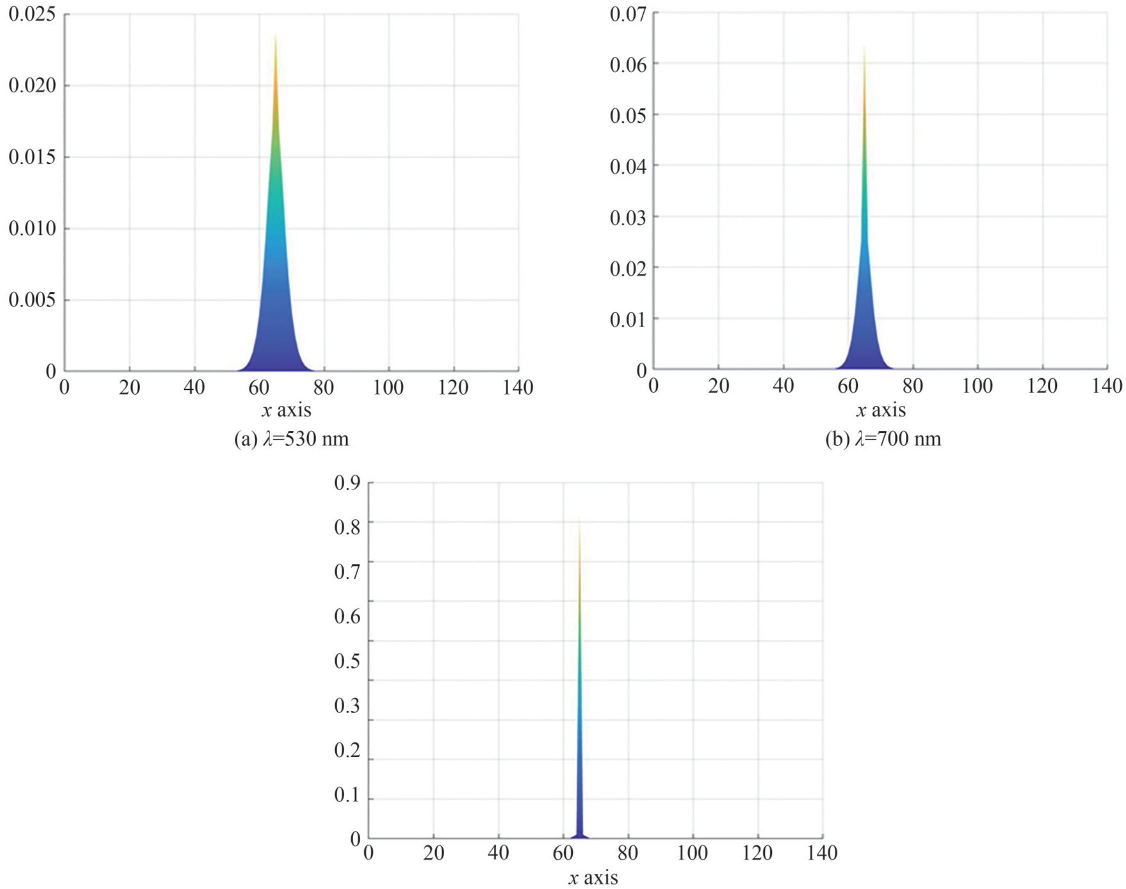

(a) λ=530 nm (b) λ=700 nm (c) λ=830 nm

图5　不同入射波长下AlGaAs窗口层粗糙表面的点扩散函数

Fig.5　Point spread function of AlGaAs surface window layer rough surface at different incident wavelengths

小,成像越清晰。

将分辨力靶图像与AlGaAs窗口层粗糙表面的点扩散函数进行卷积,获得退化后的图像如图6所示。可以看出,不同的入射光波长对应图像退化程度不同,入射光波长从530 nm增加到830 nm,图像退化后的 $PSNR_R$ 可由26.31增加到27.65,提高5.1%。即在相同的表面粗糙度下,入射光波长越长,AlGaAs窗口层粗糙表面散射对于成像质量的影响越小,退化图像与原始图像的差值越小,图像越清晰。故对于透射式NEA GaAs光电阴极而言,需要不断降低AlGaAs窗口层表面粗糙度以匹配400~900 nm波段内高分辨成像的应用需求。

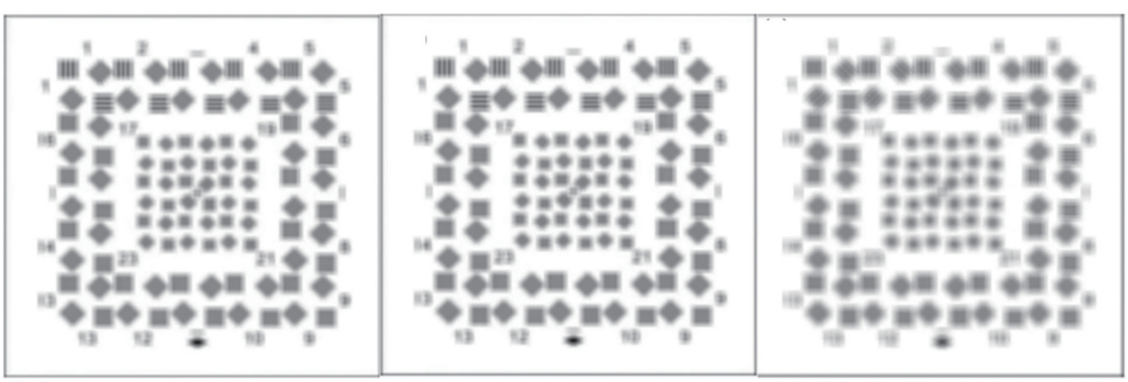

(a) λ=830 nm, $PSNR_R$=27.65 (b) λ=700 nm, $PSNR_R$=27.45 (c) λ=530 nm, $PSNR_R$=26.31

图6　不同波长下的 $PSNR_R$ 计算值

Fig.6　Calculated values of $PSNR_R$ at different wavelengths

2.3 三代微光像增强器极限分辨力测试结果

如图7所示，对理论模型进行实验验证，仪器包括光源、平行光管、成像物镜、三代微光像增强器和显微目镜等。卤钨灯发出白光，经过滤光片组并穿过平行光管后穿过测试靶并将分辨力靶图案投射在被测三代微光像增强器的GaAs光电阴极输入面，通过观察显微目镜上的线对数量得出相应的分辨力。

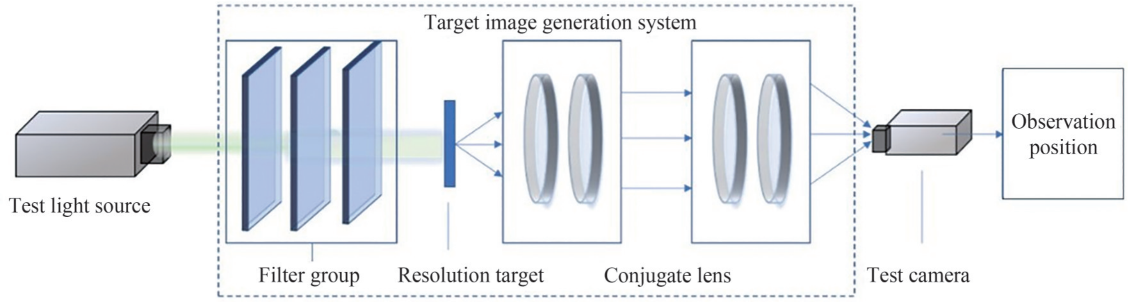

图7 分辨力实验装置

Fig.7 Resolution test device

通过调节滤光片，对同一像管进行不同波长下的分辨力测试，测试波长选择为全光谱、530 nm、830 nm，测试结果如表1所示。从实际测量结果显示全光谱下像管分辨力处于较低值，入射波长为830 nm时的分辨力值优于530 nm，该实验结果与计算结果变化趋势保持一致，证明理论计算模型精确性和泛化能力较好。

表1 不同入射波长下分辨力测试结果

Table 1 Resolution test results at different incident wavelengths

Incident wavelength/nm	Limited resolution/(lp•mm^{-1})
400～900	54
530	57
830	61

3 结论

基于散射传递函数模型，分别计算了在530 nm、700 nm和830 nm波长条件下，入射光在三代微光像增强器光阴极AlGaAs窗口层的界面散射，得到了像增强器分辨力与入射光散射的对应关系。在相同表面粗糙度条件下，850 nm波长的入射光散射传递函数所围面积最大，散射降解后的图像信噪比最高，说明入射光学图像的能量损失最小，光学图像的信息容量最高，成像质量最好。进一步通过实验对理论模型进行了验证，对同一像增强器，入射波长为830 nm时测得的分辨力优于530 nm波长的入射光，测试结果与理论计算模型结果保持一致，验证了计算模型的准确性。研究结果对于探索提高透射式NEA GaAs光电阴极的空间分辨能力有一定的参考价值。

参考文献

[1] LIU Jian, GUO Yiliang, FENG Cheng, et al. Improved preparation techniques for preparing high-performance GaAs photocathodes[J]. Applied Optics, 2020, 59(27): 8147-8151.

[2] CHRZANOWSKI K. Review of night vision technology[J]. Opto-Electronics Review, 2013, 21(2): 153-181.

[3] KARKARE S, BOULET L, CULTRERA L, et al. Ultrabright and ultrafast Ⅲ--Ⅴ semiconductor photocathodes[J]. Physical Review Letters, 2014, 112(9): 097601.

[4] FENG Cheng, ZHANG Yijun, QIAN Yunsheng, et al. Improved quantum efficiency and stability of GaAs photocathode using favorable illumination during activation[J]. Ultramicroscopy, 2019, 202: 128-132.

[5] JIN Xiuguang, OHKI S, ISHIKAWA T, et al. Analysis of quantum efficiency improvement in spin-polarized photocathode [J]. Journal of Applied Physics, 2016, 120: 164501.

[6] JIAO Gangcheng, ZHANG Kaimin, ZHANG Yijun, et al. Effect of improved 'yo-yo' Cs/O alternate activation method on stability of GaAs photocathode[J]. Acta Photonic Sinica, 2022, 51(2): 0212001.
焦岗成，张锴珉，张益军，等. 改进“yo-yo”Cs/O交替激活方法对GaAs光阴极稳定性影响[J]. 光子学报，2022，51(2)：0212001.

[7] DING Xiaojun, GE Xiaowan, ZOU Jijun, et al. Photoemission characteristics of graded band-gap AlGaAs/GaAs wire photocathode[J]. Optics Communications, 2016, 367: 149-154.
[8] QIU Yafeng, YAN Wuling, HUA Sangtun, et al. Resolution research of low-light-level image intensifier based on electronic trajectory tracking[J]. Acta Photonica Sinica, 2020, 49(12): 1223003.
邱亚峰，严武凌，华桑暾. 基于电子追迹算法的微光像增强器分辨力研究[J]. 光子学报，2020，49(12)：1223003.
[9] DENG Wenjuan, ZHU Bin, WANG Zhuangfei, et al. Resolution characteristics of varying doping and varying composition $Al_xGa_{1-x}As/GaAs$ reflective photocathodes[J]. Acta Physica Sinica, 2022, 71(15): 157901.
邓文娟，朱斌，王壮飞，等. 变掺杂变组分$Al_xGa_{1-x}As/GaAs$反射式光电阴极分辨力特性[J]. 物理学报，2022，71(15)：157901.
[10] REN Ling, CHANG Benkang, HOU Ruili, et al. Transport characteristic of photoelectrons in uniform-doing GaAs photocathode[J]. Acta Physica Sinica, 2011, 60(8): 087202.
任玲，常本康，侯瑞丽，等. 均匀掺杂GaAs材料光电子的输运性能研究[J]. 物理学报，2011，60(8)：087202.
[11] WANG Honggang, JI Xuehong, HOU Dianli, et al. Effect of electron lateral diffusion in transmission-mode varied-doping Al0.37Ga0.63N photocathode on resolution[J]. Journal of Optoelectronics and Advanced Materials, 2022, 24(1-2): 28-34.
[12] HARVEY J E, KOTHA A. Scattering effects from residual optical fabrication errors[C]. SPIE, 1995, 2576: 155-174.
[13] HARVEY J E, PFISTERER R H. Evolution of the transfer function characterization of surface scatter phenomena[C]. SPIE, 2016, 9961: 99610E.
[14] CHURCH E L. Fractal surface finish[J]. Applied Optics, 1988, 27(8): 1518-1526.
[15] MANUEL N V, NICOLAS G. A detailed study of the scattering of scalar waves from random rough surface[J]. Optica Acta: International Journal of Optics, 1981, 28(12): 1651-1672.
[16] ZHAO Jie, CHEN Zhenxue, WU Q M J, et al. Improved edge-guided network for single image super-resolution[J]. Multimedia Tools and Applications, 2022, 81(1): 343-365.
[17] LIU Qingxin, LI N, JIA Heming, et al. Modified remora optimization algorithm for global optimization and multilevel thresholding image segmentation[J]. Mathematics, 2022, 10(7): 1014.

Effect of Incident Light Scattering at AlGaAs Window Layer Interface on Resolution of Transmission-mode GaAs Photocathode

GUO Xin[1,2], SHI Feng[2], JIA Tiantian[2], ZHANG Ruoyu[2], CHENG Hongchang[2], ZHANG Yijun[3]

(1 *School of Optoelectronics, Beijing Institute of Technology, Beijing* 102401, *China*)
(2 *Science and Technology on Low-Light-Level Night Version Laboratory, Xi'an* 710065, *China*)
(3 *School of Electronic and Optical Engineering, Nanjing University of Science and Technology, Nanjing* 210094, *China*)

Abstract: Negative Electron Affinity (NEA) GaAs photocathode, as the most promising Ⅲ-Ⅴ semiconductor photocathode for low-light image intensifier, has wide applications in underwater target detection, range gated imaging, and night vision. According to the photoemission theory of transmission-mode GaAs photocathode, the incident light needs to pass through AlGaAs window layer before it can be absorbed and converted into photogenerated carriers by GaAs emission layer. The performance of image resolution on GaAs photocathode could result from the resolution of optoelectronic image and optical image. The resolution of optoelectronic image is determined by the longitudinal diffusion of photoelectrons in the emission layer. The resolution of optical image is mainly affected by the scattering of incident photons on the rough surface of the window layer. Most research on GaAs photocathode has focused on obtaining a higher optoelectronic image resolution, but there is rare research concentrated on improving the optical image resolution. However, the resolution of transmission-mode GaAs photocathode is hard to improve due to the ignorance of the optical image resolution. In order to study the image resolution of the transmission-mode GaAs photocathode under different wavelengths of incident light, a theoretical model based on the Scattering Transfer Function (STF) for the analysis of interfacial scattering from the AlGaAs window layer is proposed. A transmission-mode GaAs photocathode was fabricated, and the degradation of the incident optical image caused by the interfacial scattering of the AlGaAs window layer was quantitatively analyzed based on the signal-to-noise ratio fitting with reference peaks by using the variation of the STF and the Point Spread Function (PSF). The STF of the AlGaAs window layer rough surface under different incident light wavelengths was calculated and the incident light wavelength was set as 530 nm, 700 nm, and 830 nm respectively. The obvious characteristic is that the value of STF is improved when the incident light wavelength increases. Therefore, When the wavelength of incident light is reduced from 830 nm to 530 nm, the reduction of STF means that the area or integral value enclosed by the surface transfer function is smaller, resulting in the smaller the capacity of optical image information and the more blurred the imaging. The PSF of the AlGaAs window layer rough surface can be obtained by Fourier quasi-transform based on the STF. The results show that the central value of the PSF increases with the increase of the incident wavelength, which means the central energy of the optical image plane becomes more concentrated. In order to analyze the imaging quality of the third generation low light level image intensifier due to the scattering of incident light with different wavelengths on the rough surface of AlGaAs window layer, the PSF is convoluted with the original image of the given standard resolution target to simulate image degradation. When the incident light wavelength increases from 530 nm to 830 nm, the peak signal-to-noise ratio after image degradation increases from 26.31 to 27.65, increasing by 5.1%. Computational results indicate that under the same surface roughness, compared with the incident light with the wavelength of 530 nm, the incident light with the wavelength of 830 nm is more beneficial to obtain a larger central value of the scattering transfer function and point spread function, which means that it is more conducive to obtain a sharper incident optical image. Furthermore, when the incident light wavelength is 850 nm, the signal-to-noise ratio of the image after scattering degradation is the highest, which also shows that the energy loss of the incident optical image is the smallest, the information capacity of the optical image is the highest, and the imaging quality is the best. This work will provide a reference for developing high-performance GaAs photocathodes.

Key words: Photocathode; GaAs; Scattering transfer function; Wavelength; Roughness; Resolution

OCIS Codes: 120.4640; 160.2100; 230.0250; 290.5880; 100.2960

Foundation item: National Natural Science Foundation of China (No. 61771245), the Defense Industrial Technology Development Program of China (No. JCKY2018208B016)